Ecological Indicators 180 (2025) 114349

Contents lists available at ScienceDirect

Ecological Indicators

journal homepage: www.elsevier.com/locate/ecolind

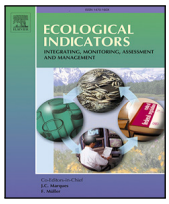

Original articles

A generalizable deep learning framework for large-scale mapping of seagrass habitats

Àlex Giménez-Romero [a,b,*], Dhafer Ferchichi [a], Pablo Moreno-Spiegelberg [a], Tomàs Sintes [a], Manuel A. Matías [a]

[a] Instituto de Física Interdisciplinar y Sistemas Complejos (IFISC, CSIC-UIB), Campus UIB 07122 Palma de Mallorca, Spain
[b] Centre d'Estudis Avançats de Blanes (CEAB-CSIC), Blanes, Girona, Spain

ARTICLE INFO

Keywords:
Seagrass monitoring
Posidonia oceanica
Deep learning
Remote sensing
Marine habitat mapping

ABSTRACT

Seagrass meadows play a vital role in supporting coastal communities by promoting biodiversity, mitigating coastal erosion, and contributing to the local economy. These ecosystems face significant threats, including habitat loss, degradation, and climate change. This has led the United Nations to recognize the urgency of conserving marine ecosystems, highlighting the need for evidence-based conservation strategies and high-quality monitoring methods. However, traditional monitoring approaches are often time-consuming, labor-intensive, and costly, limiting their scalability and effectiveness in large-scale applications. Here, we present a deep learning framework based on convolutional neural networks to identify *Posidonia oceanica* meadows in the Mediterranean Sea using satellite imagery. We demonstrate the generalization capability and robustness of the model by introducing appropriate metrics that overcome the limitations of current approaches. We show that our model is capable of providing reliable estimates of the distribution of the considered habitats and accurate measures of their extension areas. Our study contributes to the development of a reliable map of the distribution of *Posidonia oceanica* meadows in the Mediterranean Sea, showcasing the transformative potential of remote sensing and machine learning technologies for marine habitat monitoring.

1. Introduction

Coastal ecosystems, including seagrasses, mangroves, saltmarshes, and coral reefs, provide invaluable services that contribute to supporting the livelihoods of coastal communities, impacting the well-being of their residents (Millennium Ecosystem Assessment, 2005; Kallesøe et al., 2008). Seagrass meadows are crucial for enhancing coastal biodiversity by serving as essential habitats for a diverse range of marine species (Beck et al., 2001). They provide vital food, shelter, and structural support, including nursery areas for commercially important species, thereby supporting both local economies and subsistence fisheries (Heck Jr et al., 2003). Seagrass ecosystems play a crucial role in preventing coastal erosion. The dense canopies of seagrass attenuate currents and waves, facilitating particle sedimentation and mitigating sediment resuspension (Granata et al., 2001; Koch et al., 2006; Bos et al., 2007; Gacia and Duarte, 2001). Additionally, the extensive underground network of rhizomes and roots stabilizes sediment, reducing erosion and decreasing water turbidity (Madsen et al., 2001), and strongly influencing coastal sedimentary dynamics (Marbà et al., 2002; van der Heide et al., 2007). Specifically, the robust root systems of *Posidonia oceanica* beds act as natural barriers, protecting coastlines from the destructive force of strong waves and maintaining shoreline stability (Fonseca and Cahalan, 1992; Sánchez-González et al., 2011; van de Vijsel et al., 2023). In addition, seagrasses keep the overlying waters oxygenated and with low concentrations of nutrients and CO_2 (Duarte and Chiscano, 1999). Seagrasses are among the planet's most effective natural ecosystems for sequestering (capturing and storing) carbon, performing at a rate that is 35-times faster than tropical rainforests. At the same time, their sediments never become saturated (Mcleod et al., 2011). However, if these habitats are degraded, they could leak stored carbon into the atmosphere, further accelerating global warming (Duarte et al., 2013; Macreadie et al., 2014). In fact, despite the considerable uncertainty surrounding global seagrass extent values, it is estimated that approximately one-third of the worldwide seagrass extent has been lost since World War II (Duarte et al., 2013).

Seagrass decline is primarily attributed to a synergy of human-driven factors. These factors include eutrophication, where excessive nutrient runoff causes light reduction via algal overgrowth and turbidity (Burkholder et al., 2007); degradation of water quality, involving pollutants, heavy metals, and sediment loading (Zhang et al., 2023); habitat destruction, stemming from direct mechanical damage

* Corresponding author at: Instituto de Física Interdisciplinar y Sistemas Complejos (IFISC, CSIC-UIB), Campus UIB 07122 Palma de Mallorca, Spain.
E-mail address: alex.gimenez@csic.es (À. Giménez-Romero).

https://doi.org/10.1016/j.ecolind.2025.114349
Received 15 July 2025; Received in revised form 18 October 2025; Accepted 19 October 2025
Available online 1 November 2025

by coastal development, dredging, and destructive fishing or boating practices (Short and Wyllie-Echeverria, 1996); and climate change, particularly global warming, which induces thermal stress and exacerbates storm damage (Waycott et al., 2009). Furthermore, the sensitivity of seagrasses to future ocean temperatures under different emission scenarios is a significant concern. Models project a decline in the global suitable habitat for these ecosystems throughout the current century, both latitudinally and across water depths, with a notable compression of suitable habitats toward the lower distribution limit imposed by light availability (Jorda et al., 2020). In this context, the United Nations (UN) has recognized the severity of global biodiversity loss and ecosystem degradation, stressing the negative impact of this situation on food security, nutrition, access to water, the health of rural populations, and the health of people worldwide. Accordingly, the UN declared the period 2021–2030 as the "Decade of Ocean Science for Sustainable Development" and the "Decade of Ecosystem Restoration" (Waltham et al., 2022; United Nations, 2012), underlining the urgency and importance of safeguarding marine ecosystems, including *Posidonia oceanica* meadows. Achieving these targets, particularly concerning the preservation and restoration of coastal ecosystems, requires a rigorous and evidence-based approach to conservation practice and policy. This entails conducting thorough analyses of high-quality monitoring data to inform decision-making and to validate intervention strategies.

Comprehensive mapping of various marine habitats, including coral reefs, kelp forests, deep-sea vent communities, and seagrass beds, has been successfully achieved using side-scan sonar systems (Mumby and Edwards, 2002; Mishra et al., 2006; Le Quilleuc et al., 2022; Allen Coral Atlas, 2022). This methodology provides valuable insights into the structure and distribution of these ecosystems, facilitating the development of informed conservation strategies and effective management practices. However, the cost and time-intensive nature of these methods presents challenges in deploying continuous monitoring systems in marine environments. As a result, practical monitoring of biodiversity often occurs infrequently rather than in real-time, preventing a constant spatiotemporal evaluation of the status of these ecosystems. A recently emerging possibility is to combine remote sensing technologies with available georeferenced habitat data to develop correlative or mechanistic models that can be used to monitor biodiversity at finer temporal scales. Among the various methodologies, Machine Learning (ML) models trained with multispectral satellite imagery data appear to be the most promising (Zhang et al., 2013; Senecal et al., 2019; Wicaksono et al., 2019; Gudžius et al., 2021).

In recent years, a range of studies have explored machine-learning and remote-sensing approaches to map *Posidonia oceanica* and other Mediterranean benthic habitats. Drone-based work has shown excellent classification accuracy at very fine spatial scales but is necessarily local in extent and seasonally constrained (Kellaris et al., 2019; Chand and Bollard, 2022; Jeon et al., 2021). Sentinel-2 studies have demonstrated the value of freely available multispectral data (Traganos et al., 2018; Ha et al., 2020; Traganos and Reinartz, 2018b), but they also highlight sensor-specific artifacts and limitations (e.g., striping, coarse spectral and spatial resolution, and sensitivity to atmospheric/aerosol correction) that complicate operational mapping in optically shallow waters (Traganos and Reinartz, 2018a; Poursanidis et al., 2019). Several regional studies based on multispectral satellite imagery or a small set of images report high overall accuracies, yet rely on a limited number of acquisition dates and on photo-interpreted ground truth with sparse field validation, which reduces confidence in model robustness and hampers transferability (Traganos et al., 2018; Marcello et al., 2018; Traganos and Reinartz, 2018b; Coffer et al., 2020). Methodologically, many applied studies use conventional classifiers (e.g., Random Forests, SVMs) or simple two-class schemes that conflate ecologically distinct substrates, which can inflate apparent performance while failing to capture fine benthic heterogeneity (Poursanidis et al., 2018; Traganos and Reinartz, 2018b; Traganos et al., 2018; Traganos and Reinartz, 2018a; Marcello et al., 2018; Poursanidis et al., 2019; Ariasari et al., 2019; Ha et al., 2020). Indeed, there is recent evidence on the unreliability of SVM classifications (Bakirman and Gumusay, 2020). The predominance of conventional classifiers in this field is striking, given that convolutional neural networks (CNNs) have become the state of the art for a wide range of image-based deep learning (DL) applications over the past decade, including object recognition, pattern detection, and semantic segmentation. Unlike pixel-wise approaches such as Support Vector Machines or Random Forests, CNNs jointly exploit spectral information and spatial context, enabling them to detect boundaries, textures, and neighborhood relationships that are particularly relevant in heterogeneous coastal environments. By capturing both local features and larger spatial structures, CNNs achieve substantially higher accuracy in complex segmentation tasks (Zeiler and Fergus, 2014; Milletari et al., 2016). Despite these clear advantages, however, simpler classifiers still dominate applications to seagrass habitat mapping. Finally, recent DL-based work does not report segmentation-specific metrics (such as Intersection-over-Union) and instead relies on overall accuracy or user and producer accuracies (Chowdhury et al., 2024), a practice that can overestimate model performance in spatially structured segmentation tasks.

In this work, we overcome current limitations by developing a CNN-based framework that moves beyond local proof-of-concepts toward robust and operational mapping tools. We train convolutional neural networks that jointly exploit spectral and spatial context, benchmark performance with segmentation-appropriate metrics (Intersection over Union and spatially explicit error estimates), use an extensive field-validated habitat dataset rather than relying solely on photo-interpretation or sparse field data, and explicitly test transferability/generalizability by training on one island and evaluating predictions on several ecologically distinct islands. Three key considerations guide our approach. First, the georeferenced habitat dataset was acquired using a consistent methodology and covering a broad geographical area across multiple spatial scales, thereby capturing diverse ecological conditions. Second, we train deep learning models on a heterogeneous set of satellite images that incorporate variability in acquisition dates, geographic locations, and Sun–satellite geometry, ensuring that the models learn under realistic conditions and are robust to natural sources of variation. Finally, we evaluate the model's generalizability and predictive performance on regions geographically distinct from the training dataset, characterized by different environmental and community structures, to demonstrate its applicability across varied real-world scenarios.

2. Methods

2.1. Satellite data

Satellite imagery was obtained from Planet under the Education and Research Program, which provides limited non-commercial access to PlanetScope and RapidEye imagery (Planet Team, 2017). In particular, we acquired PlanetScope images obtained through the Super Dove (PSB.SD) instrument, which consists of Coastal Blue, Blue, Green I, Green, Yellow, Red, Red Edge, NIR, and operates from 2020. Surface Reflectance (SR) products were selected to ensure consistency across localized atmospheric conditions, minimizing uncertainty in spectral response across time and location. SR is derived from the standard Analytic Product (radiance), which is processed to top-of-atmosphere reflectance and then atmospherically corrected to bottom-of-atmosphere reflectance. For submerged vegetation, near-infrared bands are rapidly absorbed by the water column and provide little signal, so discrimination among classes relies primarily on the rest of the spectrum (see Supplementary Fig. 2 for class-specific spectral responses).

We obtained 60 satellite images along the coast of the Balearic Islands, covering a surface area of up to 1200 km^2 for the years 2020 to 2023 (see Supplementary Information, Supplementary Fig. 1). The images were acquired over several days under clear sky conditions,

ranging from June to September, as these are the months when the biomass of seagrass and algae is most abundant. No other filters were applied to the images, as we aimed to train the model in real-world scenarios, where one cannot control for specific environmental conditions, constrained dates for image acquisition, and the satellite's position with respect to the Sun and the Earth, among other factors. Thus, we obtained images under different conditions (see Supplementary Information, Supplementary Table 1). This variability introduces heterogeneity in the training and testing data, reflecting the range of conditions encountered in real-world applications. For example, habitat composition differs among islands: *Zostera noltii* occurs only in Menorca, "mud" substrates are present only in Ibiza, and "coarse sands" appear in Ibiza and Formentera but not in Mallorca (Supplementary Table 2). Thus, ecological and environmental conditions vary substantially across the study area, and by deliberately including this variability in our dataset, we aim to develop models that retain predictive skill across distinct settings, rather than being optimized for standardized conditions.

2.2. Habitat data

We used georeferenced habitat data from the Government of the Balearic Islands, which corresponds to the outcome of various European and national projects, encompassing a ~20-year effort in data acquisition covering a total of 2500 km^2 (Goverment of the Balearic Islands, 2000-2019; del Valle Villalonga et al., 2023). The first project commenced around 2000, and a significant update was implemented in 2018. The data consist of 28 different habitat classes following the nomenclature and coding of the Standard List of Marine Habitats of Spain (LPHME), obtained from side scan sonar, photo-interpretation of airborne imagery, and in situ observations. We aggregated the different habitat classes into four major ecological groups that are present throughout the Mediterranean Sea. The aggregation was based on feature similarity and ecological function, resulting in the following classes: Posidonia oceanica, green algae, brown algae, and rocks, and sandy bottoms (see Supplementary Information, Supplementary Table 2).

Fig. 1a shows the spatial distribution of the considered ecological groups in the Balearic Sea. This comprehensive dataset provides detailed information at multiple spatial scales, offering valuable insights into the intricate spatial patterns of different habitat classes across the region. The detailed information captured by the high-resolution data contributes significantly to the reliability of our model and the precision of our predictions, which are particularly vital in the context of habitat conservation for *Posidonia oceanica* meadows.

2.3. Bathymetry data

Bathymetry data were obtained from the European Marine Observation and Data Network (EMODNET) (Martín Míguez et al., 2019). EMODnet Bathymetry provides a service for viewing and downloading a harmonized Digital Terrain Model (DTM) for European sea regions. The data consist of GeoTIFF layers with ~100 m pixel resolution of mean depth values, which were interpolated to the satellite imagery resolution.

2.4. Dataset creation

Satellite images were processed with habitat and bathymetry data to construct the final training and testing datasets. The NIR band, which is strongly attenuated by water, was used to mask out pixels corresponding to land using a simple clustering algorithm (namely K-means) and subsequently replaced by bathymetry data. The resulting processed satellite images served as the primary source of input data for our model. The ground truth (or label) dataset consists of raster files analogous to satellite images with single-band values representing the benthic class corresponding to each pixel. To construct it, all pixels of each processed satellite image were associated with a given benthic class using aggregated habitat data. Pixels for which a class was not available were masked out in both the processed satellite images and label data. Similarly, the pixels already masked in the satellite image were kept masked in the label image. Finally, patches measuring 256 × 256 pixels (~750 m × 750 m) were extracted from each satellite and label image for the years 2020 to 2022 (with 2023 reserved as a final test), resulting in a final dataset comprising up to 16,430 patches.

Despite the train-test data split usually following an 80%-20% ratio, training was conducted exclusively with data from Mallorca (8488 patches, of which 1698 were allocated for validation), and testing was performed with the remaining data from Menorca, Ibiza, Formentera, and Cabrera islands (7942 patches), resulting in a roughly 50%–50% train-test split. Furthermore, our test set represented diverse environmental conditions and even benthic habitats formed by slightly different species than the training set, thereby simulating real-world scenarios that the model may encounter in operational settings. By testing the model on data from regions beyond its training domain, we aimed to assess its generalization and robustness. Specifically, we sought to determine whether the model could accurately classify marine habitats and benthic features in unseen environments, which are likely to differ slightly from those in the training data, thereby demonstrating its capacity for real-world application. We refer to our test set as an "out-of-sample" test set to emphasize this idea.

Finally, all images from 2023, covering the coasts of all the islands, were selected for a final test set to analyze model robustness once it is trained on data from all regions from 2020 to 2022.

2.5. Deep learning models

We trained various state-of-the-art deep learning models for semantic image segmentation, including UNET (Ronneberger et al., 2015), LinkNet (Chaurasia and Culurciello, 2017), FPN (Lin et al., 2017), and PSPNet (Zhao et al., 2017). Each architecture is formed by repeating convolutional blocks, which are usually referred to as the "backbone" of the model. We tested ten different backbone models for each architecture, resulting in the training and evaluation of 40 deep learning models, which represents an unprecedented effort in the field. We used the segmentation-models Python library (Iakubovskii, 2019) to define and train all the models.

2.6. Model training

Before training, the input data was standardized using the mean and variance of the training data,

$$z = \frac{X - \mu}{\sigma} . \quad (1)$$

This standard scaling procedure ensures that all input features have a consistent scale, preventing the dominance of specific features during the training process. It is crucial to note that the same standard scaling procedure must be applied during predictions using the mean and standard deviation calculated from the training set. This consistency ensures that the model interprets new data in a comparable manner to the training data.

Additionally, because the output was categorical, the labels were one-hot encoded. This encoding converts categorical labels into binary vectors, where each class is represented by a unique binary value, facilitating the model's interpretation of the multi-class classification task.

For the loss function, we opted for the dice loss owing to its effectiveness in handling imbalanced datasets, which is a common characteristic in tasks involving semantic segmentation (Rahman and Wang, 2016). Dice loss, also known as the Sørensen–Dice coefficient (Sorensen, 1948; Dice, 1945), measures the similarity between predicted and ground truth data by computing the intersection over the

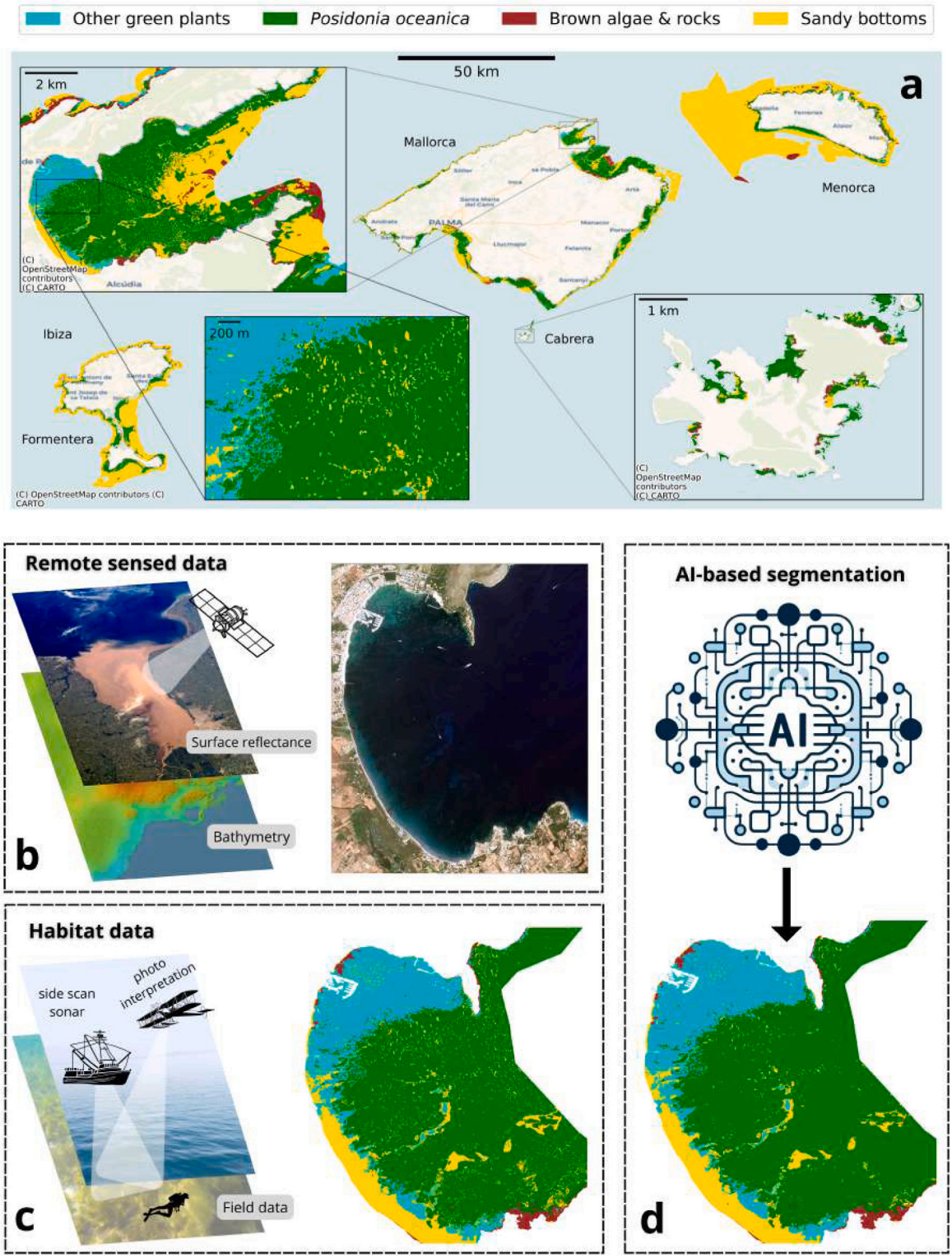

Fig. 1. (a) Spatial distribution of the four main ecological benthic habitats in the Balearic Sea, present in the whole Mediterranean. The dataset provides detailed information at multiple spatial scales, with a resolution of up to 3 m. (b–d) Scheme of the pipeline used to train the CAMELE model. (b) Satellite-based surface reflectance data were merged with bathymetry estimates to produce the model inputs (features). (c) Habitat data obtained with side-scan sonar, photo-interpretation, and field observations were used as ground truth data (labels). (d) These features and labels are used to train deep convolutional neural networks to perform image segmentation. (For interpretation of the references to colour in this figure legend, the reader is referred to the web version of this article.)

union of the two. To further account for class imbalance, we applied loss weights that were inversely proportional to the proportion of examples of each class. The learning rate was set to 0.001 to ensure a smooth training process.

The models were trained on a computing cluster utilizing 10 cores and a maximum of 400 GB of RAM per model. The training process was performed for 1000 epochs, with a batch size of 32. The total training time was approximately one month for the 40 initial models, which

used data from the island of Mallorca, and approximately three months for the 10 final models, which used all available data.

2.7. Performance metrics

The performance of our trained models was primarily evaluated using the Intersection over Union (IoU) score (Eq. (7)), which measures the spatial overlap between the predicted image and the ground truth, as this metric is suitable for image segmentation problems (Rahman and Wang, 2016). Additionally, we considered other metrics such as accuracy (Eq. (2)), precision (Eq. (3)), recall (Eq. (4)), F-1 score (Eq. (5)) and Cohen's Kappa (Eq. (6)) to perform a comprehensive evaluation of the model. Accuracy gauges the overall correctness of the predictions, whereas precision measures the accuracy of positive predictions. Recall assesses the model's ability to capture all positive instances, and the F-1 score provides a balanced assessment of precision and recall. For a binary classification problem, the metrics can be defined using a confusion matrix, where TP, TN, FP, and FN represent true positives, true negatives, false positives, and false negatives, respectively. N represents the total number of pixels in the image.

$$\text{Accuracy} = \frac{TP + TN}{N} \tag{2}$$

$$\text{Precision} = \frac{TP}{TP + FP} \tag{3}$$

$$\text{Recall} = \frac{TP}{TP + FN} \tag{4}$$

$$\text{F1 Score} = \frac{2 \times TP}{2 \times TP + FN + FP} \tag{5}$$

$$\kappa = \frac{2(TP \times TN - FP \times FN)}{(TP + FN)(FN + TN) + (TP + FP)(FP + TN)} \tag{6}$$

$$\text{IoU} = \frac{|P \cap L|}{|P \cup L|} = \frac{TP}{TP + FP + FN} \tag{7}$$

These metrics collectively provide a comprehensive understanding of the model's effectiveness in classifying benthic habitats. Please refer to the Supplementary Information for further details.

2.8. Consensus prediction

We implemented a consensus prediction approach to enhance the robustness and reliability of the model predictions. The consensus prediction involved aggregating the results from multiple deep learning models, each trained with different architectures and backbones. By combining predictions from diverse models, we aim to mitigate the potential biases introduced by individual models and enhance the overall accuracy and generalization capabilities of the ensemble.

For each input patch, predictions from all the trained models were collected, and a voting mechanism was employed to determine the final consensus prediction. Specifically, the class label with the highest frequency across all the model predictions was assigned to each pixel. This ensemble-based strategy leverages the diversity of information captured by different models, leading to more robust and reliable classification outcomes.

2.9. Model selection

To filter among the four different architectures, we evaluated the performance of the models using the training dataset. Despite all models achieving high IoU scores (>0.8), LinkNet and UNET architectures were the best-performing models, with mean IoUs of 90.98% and 90.90%, respectively (Supplementary Table 3). Because the LinkNet architecture has fewer trainable parameters than UNET, it is more efficient in terms of computational resources and is less prone to overfitting. Therefore, we selected it as the final architecture to build CAMELE, which ultimately consists of ten different models (Supplementary Information).

We then evaluated the performance of each of the 10 models and the consensus prediction approach in the training and out-of-sample test datasets. All models achieved high performance, with a median IoU of 88.12% and F1-score of 93.16% in the training dataset (Supplementary Table 5). In contrast, the models' performance in the out-of-sample test dataset was significantly reduced, with a median IoU of 60.73% and F1-score of 71.87% (Supplementary Table 6). When analyzing the performance of the models individually, we observed the emergence of "specialists", which performed significantly better than the rest of the models for segmenting specific classes. This finding underscores the importance of the consensus prediction approach, which leverages the diversity of information captured by various models. The consensus prediction approach significantly improved the models' performance in the out-of-sample test dataset, with an IoU score of 61.97% and an F1-score of 72.77% (Supplementary Table 6), highlighting the effectiveness of the ensemble-based strategy in mitigating potential biases introduced by the individual models and enhancing the overall accuracy and generalization capabilities of CAMELE. Thus, the consensus prediction approach was selected as the final model for CAMELE prediction.

2.10. A deep learning framework for automated marine ecosystem labeling

We developed a deep learning framework based on convolutional neural networks to accurately classify benthic habitats in the Mediterranean Sea using satellite imagery (Fig. 1). We used a comprehensive and extensive habitat dataset of the Balearic Sea, comprising a 20-year effort of data acquisition based on side-scan sonar, supported by the photo-interpretation of high-resolution airborne imagery and in situ observations (Fig. 1a). The dataset covers approximately 2500 km^2 of the coastal habitats of the Balearic Islands at a high spatial resolution. It contains 28 different classes, including the ecologically significant species *Posidonia oceanica*, which were aggregated into four major ecological groups: "Posidonia oceanica", "Other green plants", "Rocks & brown algae", and "Sandy bottoms" (Fig. 1a,c, Methods & Supplementary Information). This dataset was combined with satellite imagery of the coastal areas of the Balearic Islands acquired from PlanetScope (Planet Team, 2017), covering around 1200 km^2 with different dates and satellite positions (Fig. 1b,c, Methods, and Supplementary Information).

We trained 40 different deep learning models using four different state-of-the-art architectures and 10 different backbones for each architecture (Fig. 1d, Methods & Supplementary Information). Furthermore, we implemented a consensus prediction approach to enhance the robustness and reliability of model predictions, which involves aggregating the results from multiple deep learning models to mitigate the potential biases introduced by individual models (Methods & Supplementary Information). To evaluate the models, we opted to train only with data from one island (Mallorca) and then conducted a systematic analysis of its performance on the other islands (Menorca, Ibiza, Formentera, and Cabrera) in an a posteriori analysis. Thus, the train-test split was roughly 50%-50% rather than the traditional 80%-20% split, with the test set representing diverse environmental conditions and benthic habitats formed by slightly different species than the training set (Methods & Supplementary Information). This approach was chosen to simulate real-world scenarios, in which one cannot control for specific environmental conditions, constrained dates for image acquisition, the position of the satellite with respect to the sun and the Earth, or even find new species that are not contained in the original training dataset. We thereafter refer to our test set as an "out-of-sample" test set and to the model as "Half model" to emphasize this idea.

We performed an extensive evaluation of the models' performance in both the training and out-of-sample test datasets using a variety

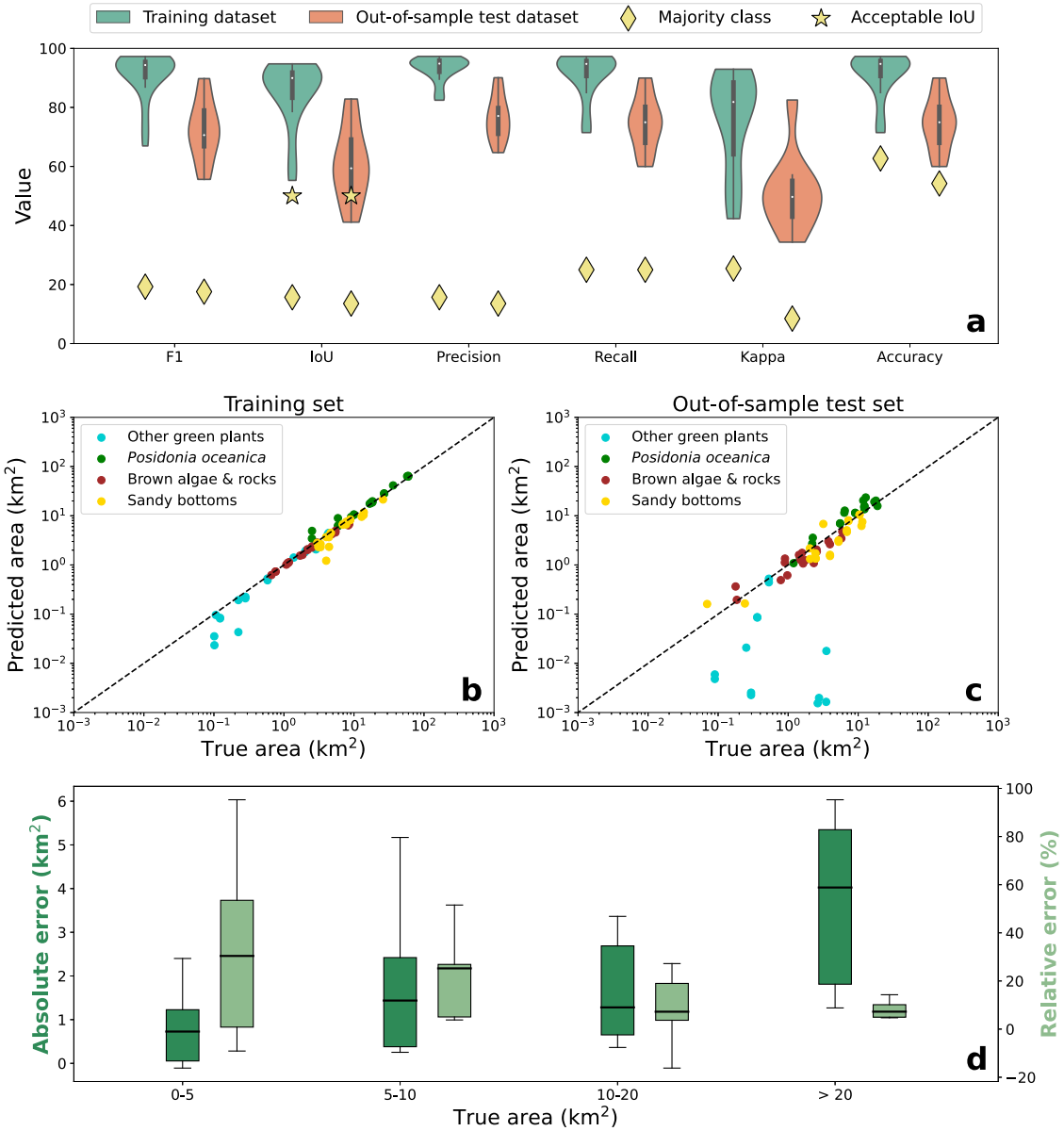

Fig. 2. Model performance in train and out-of-sample test datasets. (a) Violin plots for F1-score, IoU, Precision, Recall, Kappa, and Accuracy in both the training and out-of-sample test datasets. (b–c) True vs. predicted area for each habitat class in the training (b) and out-of-sample test (c) datasets. The diagonal dashed line indicates a perfect prediction. (d) Box plot of the absolute and relative errors in the prediction of the *Posidonia oceanica* area as a function of the true area. Relative errors decrease significantly with the extent of the area to be predicted, which is linked to the wider spatial context available. (For interpretation of the references to colour in this figure legend, the reader is referred to the web version of this article.)

of metrics, including Intersection over Union (IoU), Precision, Recall, F1-score, Kappa, and Accuracy (Methods). Our results show that the best-performing framework was to use the 10 models defined by the Linknet architecture, together with the consensus prediction approach (Methods and Supplementary Information), which hereafter we refer to as CAMELE (Consensus for Automated Marine Ecosystem Labelling and Evaluation).

3. Results

3.1. A reliable AI-based solution for marine ecosystem monitoring

CAMELE's performance in both training and out-of-sample test datasets was highly notable, with a mean IoU score of 88.22% and a mean F1-score of 93.13% in the training dataset, compared with a mean IoU score of 61.97% and a mean F1-score of 72.77% in the out-of-sample test dataset (Fig. 2a, and Supplementary Tables 5 and 6). In image segmentation tasks, an IoU score greater than 50% is considered an acceptable prediction (Dai et al., 2016) (yellow stars in Fig. 2a). Furthermore, the model outperforms the naive baseline of predicting only the majority class (yellow diamonds in Fig. 2a) by a significant margin. We observe an overlap between the distribution of the performance metrics in the training and out-of-sample test datasets, showing that model performance is consistent in both sets (Fig. 2a). The model was able to segment some images in the out-of-sample test dataset with notable performance (e.g., 15% of the images with an IoU score higher than 80%, and 20% of the images with an IoU score higher than 70%), while only 10% of the images had an IoU score lower than 50% (Fig. 2a and Supplementary Table 8). This demonstrates that the model can generalize to some extent to new regions with different environmental conditions and the presence of different benthic habitats.

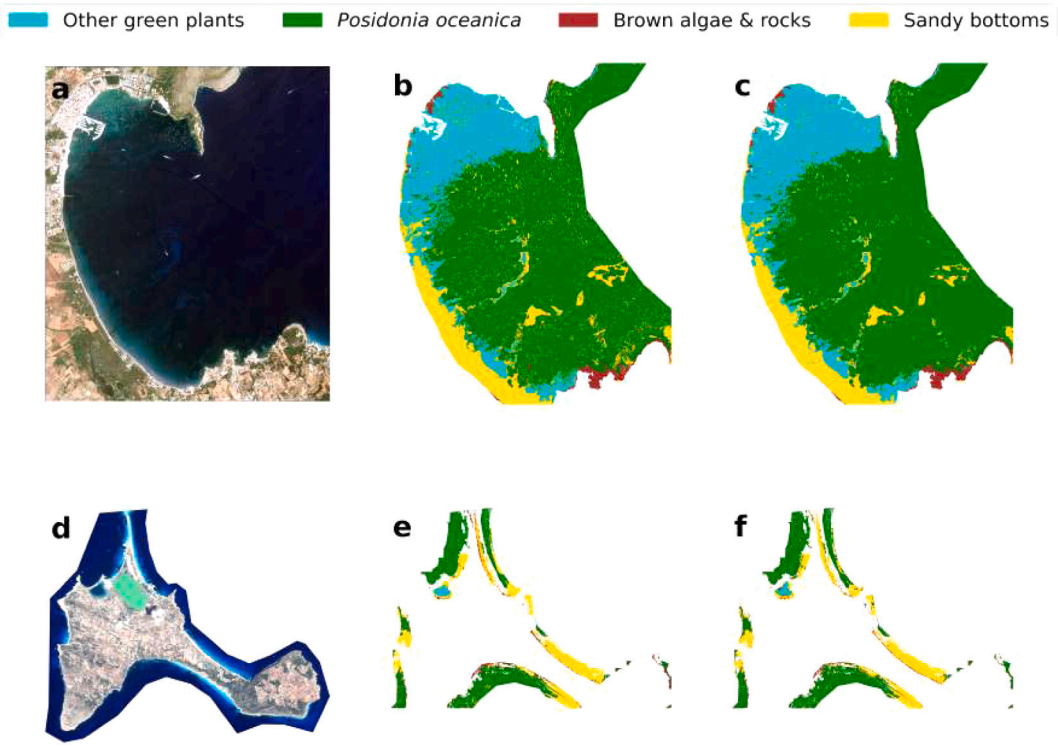

Fig. 3. Example of model predictions for a satellite image in the training and out-of-sample test set. (a) Satellite image from Pollença bay in the island of Mallorca, a part of the training set. Image © 2022 Planet Labs PBC (b) Ground truth data for the benthic habitats in Pollença bay. (c) Habitat classification from the CAMELE model in Pollença bay (92.78% IoU). (d) Satellite image from Formentera Island, part of the out-of-sample test set. Image © 2022 Planet Labs PBC (e) Ground truth data for the benthic habitats in Formentera. (f) Habitat classification from the CAMELE model in Formentera (82.54% IoU).

Despite the decrease in performance in the out-of-sample test dataset, which can be attributed to the different environmental conditions, including the presence of different benthic habitats, we observed that a significant part of the pixels categorized by the ground truth data as the model was classifying "Other green plants", "Brown algae & rocks", or "Sandy bottoms" as *Posidonia oceanica*, substantially affecting the overall performance (Supplementary Information, Supplementary Fig. 3). Surprisingly, we found that the reflectance distribution of the "Other green plants" class in the test dataset was much more similar to that of the "Posidonia oceanica" class in the training set than to its own class (Supplementary Information, Supplementary Fig. 4). Then, it is not surprising that the model classifies all those samples as *Posidonia oceanica*. In contrast, the model achieved notable performance in segmenting the Posidonia oceanica class, with a mean IoU of 77.30%, compared to the mean IoU of 91.97% achieved in the training dataset (Supplementary Table 7). At any rate, the model still achieved an overall notable performance in the out-of-sample test dataset, demonstrating the generalization capability and robustness of CAMELE and highlighting its potential for real-world applications in biodiversity monitoring and management.

CAMELE's performance was further evaluated by comparing the true and predicted areas for each habitat class in each image of the training and out-of-sample test datasets. The model achieved notable performance in predicting the area of the different habitat classes, except for the "Other green plants" class, as expected from the previous analysis (Fig. 2b,c). Specifically, the median absolute errors committed in the prediction of the area of the different habitat classes were 0.98 km^2, 0.06 km^2, 0.15 km^2, and 0.70 km^2 in the training dataset, compared with 2.24 km^2, 0.26 km^2, 0.47 km^2, and 1.12 km^2 in the out-of-sample test dataset, for the "Posidonia oceanica", "Other green plants", "Rocks & brown algae", and "Sandy Bottoms" classes, respectively. However, the relative errors were 5.61%, 11.77%, 6.77%, and 14.34% in the training dataset, compared with 24.92%, 99.20%, 28.16%, and 35.05% in the out-of-sample test dataset. The high relative errors for the "Other green plants" class in the out-of-sample test dataset are nonsensical, as the true area of this class is small, leading to a high relative error. Thus, we observed that the absolute errors doubled in the out-of-sample test dataset, whereas the relative errors increased by a factor of five. The models' performance in predicting the area of the Posidonia oceanica class was particularly notable, with relative errors significantly decreasing with the extent of the area to be predicted, linked to the broader spatial context available (Fig. 2d). For instance, the median relative error for true extent areas between 1 and 5 km^2 was 30% (86% for 95% confidence interval) compared with 7% (13% for 95% confidence interval) for areas larger than 20 km^2. This finding underscores the importance of considering the spatial context when predicting the area of benthic habitats, highlighting the potential of CAMELE to provide reliable estimates of the distribution and extension of the considered habitats in the Mediterranean Sea.

To further illustrate the model's performance, we present an example of model predictions for a satellite image in the training and out-of-sample test sets (Fig. 3). The model accurately classified the different benthic habitats in both cases, with IoU scores of 92.78% and 82.54%, respectively, providing reliable estimates of the distribution and extent of the considered habitats. We note that although there is a 10-point difference in the IoU score between each prediction, this is almost unobservable in the visual inspection of the projections, highlighting the extreme sensitivity of this metric to minor differences.

3.2. Toward a comprehensive model for the Mediterranean Sea

Finally, we trained CAMELE using all available data (13 144 patches for training and 3286 for validation) and provided our final trained models to the scientific community, which are freely accessible at Giménez-Romero (2024b). We refer to this model as the "final" model. We evaluated the performance of the final model on the complete

Table 1
Performance (IoU score) of the final model in the complete dataset and comparison with the previous model performance and previous data splits confirming the training and out-of-sample (OOS) test datasets.

	Train (Half model)	OOS test (Half model)	Complete dataset
Half model	88.22	61.97	79.21
Final model	94.73	96.22	95.22

dataset and, for comparison, also on the previous training and out-of-sample test datasets, achieving median IoU scores of 95.22%, 94.73%, and 96.22%, respectively (Table 1). Notably, the model segmented all images in the complete dataset with an IoU score higher than 90%, achieving mean, median, and maximum IoU scores of 94.64%, 95.22%, and 98.5%, respectively (Supplementary Table 10). Finally, we assessed the model's robustness by predicting on a new set of images from the Balearic Islands in 2023 that were not used in the training or out-of-sample test datasets. The model achieved a remarkable mean IoU score of 80% on this new dataset (Supplementary Table 11).

In Fig. 4, we present some examples of model predictions in different regions of the Balearic Islands, showing the ground-truth data for the benthic habitats. The habitat classification from the "CAMELE (half data)" model was trained using only half of the data (from Mallorca Island). In contrast, the habitat classification from the "CAMELE (full data)" model was trained using all available data. We observed that the main differences between the predictions of the two models occurred in areas with more complex habitat distributions. In these areas, the model trained with all available data can capture the complexity of habitat distribution more accurately, providing a more detailed and reliable classification of benthic habitats. In any case, the model trained only with data from Mallorca still provided notable performance in segmenting the *Posidonia oceanica* meadows from the other islands, which is ultimately the most essential habitat to be monitored. A web-based application for interactively visualizing all model predictions, together with the ground truth data, is available at Giménez-Romero (2024a).

4. Discussion

Despite the advancements and potential of our study, several challenges and limitations remain. First, the reliance on satellite imagery for habitat classification presents inherent limitations, including cloud cover, atmospheric interference, and limited spatial and spectral resolution, which may impact the accuracy and detail of habitat classification, especially in complex coastal environments (Mumby and Edwards, 2002; Boyle et al., 2014; Wilson et al., 2022; Doughty et al., 2024). Additionally, the availability and quality of training data pose challenges, as incomplete or biased datasets can affect model performance and generalization capabilities. Moreover, our analysis focused on four major aggregated ecological groups, including *Posidonia oceanica* habitats, neglecting other critical benthic species and ecosystems that contribute to the overall marine biodiversity. In any case, our aggregation is consistent with previous studies (Fornes et al., 2006). Furthermore, while our models exhibit robustness in cross-regional generalization within the Balearic Islands, their applicability to other geographical regions with distinct environmental conditions remains to be tested. Thus, it may have limitations in delineating finer-scale habitat features in areas with different ecological characteristics. Addressing these limitations through continued data collection, model refinement, and validation efforts is crucial for advancing the reliability and applicability of remote-sensing-based approaches in marine habitat monitoring and conservation. In addition, emerging machine learning techniques are being developed to enhance the generalizability and transferability of CNN-based mapping models (Islam et al., 2019), and integrating such advances will be important for extending the applicability of our framework beyond the Balearic Islands.

A key limitation of satellite-based seagrass mapping is the detection of meadows at greater depths, where light attenuation reduces the spectral signal available to the sensor and progressively constrains classification accuracy. This challenge is commonly addressed by applying water-column correction algorithms to compensate for absorption and scattering and to approximate the true reflectance of the seafloor (Yang et al., 2010; Zoffoli et al., 2014). However, recent work has shown that machine-learning models without explicit corrections can outperform those relying on them (Mederos-Barrera et al., 2022). In our study, we did not apply explicit corrections but included bathymetry as an additional input variable. Model tests with and without bathymetry demonstrated that performance improved substantially when depth was provided, yielding reliable estimates up to 20 m—a depth range consistent with other mapping studies (Kobryn et al., 2013; Lyons et al., 2020). This suggests that CNNs may implicitly learn to compensate for depth-related spectral attenuation. Nonetheless, a limit to detectability is expected: in our case, performance declined beyond 20 m, although this may partly reflect the smaller amount of training data available at those depths. Further research is needed to systematically assess the depth limits of deep learning models, and in particular to determine whether they can extend reliable predictions down to ~50 m, the lower bound of the natural bathymetric range of *P. oceanica* (Telesca et al., 2015).

Another limitation of our framework is that the models were trained on images acquired between June and September, when the biomass of *P. oceanica* is maximal and the meadows are most easily distinguished from algal cover. Consequently, the models are not currently suitable for continuous year-round monitoring, since seasonal phenological changes alter the spectral response of the meadows and would require season-specific training. This limitation is less critical for tracking long-term dynamics, given that the growth of *P. oceanica* is extremely slow (centimetres per year), making annual mapping sufficient to capture ecologically meaningful changes in extent. However, seagrass loss can occur much more rapidly, and in such cases, more frequent monitoring would be desirable. Future research may therefore explore the development of seasonal model ensembles or transfer-learning strategies to extend predictions across seasons. Such efforts could also be complemented with region-specific drone-based surveys, which together could provide finer-scale and more timely detection of local seagrass decline.

Beyond mapping the extent of *P. oceanica*, our framework provides outputs that can be directly used to extract spatial metrics relevant for conservation. These include measures of fragmentation (e.g., number of patches or patch size distribution) and the spatial arrangement of meadows relative to other benthic classes. For instance, the interfaces between "Posidonia oceanica" and "Other Green Plants" classes are of particular ecological interest, since this category often includes *Cymodocea nodosa* and macroalgal assemblages that can compete with or displace seagrass (Llabrés et al., 2023). Previous studies have shown that higher patchiness is associated with stronger anthropogenic pressure (Montefalcone et al., 2010; Swadling et al., 2023) and that small or fragmented patches of *P. oceanica* tend to exhibit reduced productivity and canopy height, especially under grazing pressure (Gera et al., 2013). Although we have not attempted to validate such relationships directly, our segmentation maps provide the raw material to quantify these structural attributes at broad spatial scales. Combining such information with ecological survey data could help diagnose early degradation processes and develop complementary indicators of meadow condition. In this sense, our framework has potential applications for conservation practice by delivering spatially explicit, reproducible, and open-access maps of seagrass distribution. These maps can support managers in identifying priority areas for protection and restoration, detecting hotspots of habitat loss or fragmentation, and comparing regions under different levels of anthropogenic pressure. Finally, because our trained models are openly shared, other researchers and practitioners can adapt them to new regions, thereby extending their utility beyond the Balearic Islands and supporting

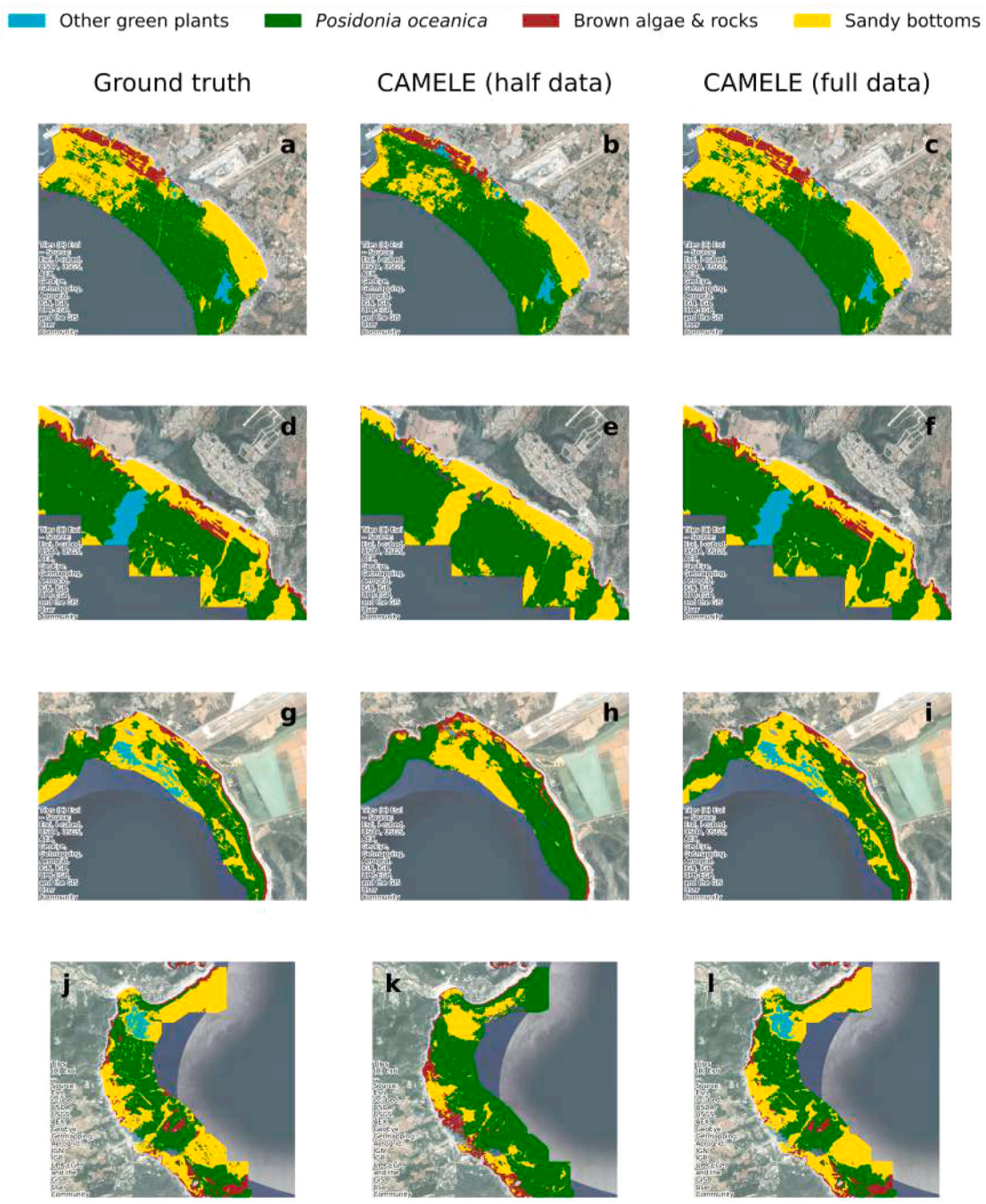

Fig. 4. Example of model predictions for a satellite image in the complete dataset. The first column shows the ground truth data for the benthic habitats, the second column shows the habitat classification from CAMELE model trained only with half of the data (from Mallorca island), and the third column shows the habitat classification from the CAMELE model trained with all available data. (a–c) Palma Bay, Mallorca. (d–f) Son Bou beach, southeast of Menorca. (g–i) Es Còdols, south of Ibiza. (j–l) Cala San Vicente, east of Ibiza.

conservation strategies across the Mediterranean and other seagrass ecosystems worldwide.

Several avenues for future research and practical applications emerge from our study. Continued efforts to expand and refine training datasets by incorporating data from diverse geographic regions and ecosystem types will further enhance the accuracy and generalization capabilities of machine learning models for marine habitat monitoring. In addition, ongoing advancements in remote sensing technology, including the development of higher spatial and spectral resolution sensors, hold promise for improving habitat classification accuracy and detail. The integration of emerging techniques, such as drone-based imaging (Kellaris et al., 2019; Chand and Bollard, 2022; Jeon et al., 2021) and LiDAR (Amani et al., 2022), further expands the scope and resolution of habitat monitoring efforts, enabling finer-scale analysis and management. Another promising extension is the development of AI models capable of detecting bleaching in *Posidonia oceanica*. This phenomenon, which has been recently observed in warm locations across the Mediterranean Sea, is characterized by the discoloration or loss of chlorophyll and carotenoid photopigments in the leaves still attached to the shoots (Stipcich et al., 2025a,b). Research is currently conflicted on whether the event is symptomatic of severe thermal stress—with some studies showing a clear correlation between maximum daily temperature and the bleached area (Stipcich et al., 2025a)—or if temperature and irradiance are not the main drivers,

pointing instead to other unknown factors (Stipcich et al., 2025b). Furthermore, it remains unclear whether bleaching is definitively detrimental to the plant's health or if it is an adaptive strategy; while it involves the loss of photosynthetic pigments, compensatory increases in total leaf area and high potential for meadow recovery have also been documented (Stipcich et al., 2025a). In any case, given the strong spectral signature resulting from the loss of pigments, integrating these insights into remote-sensing frameworks could allow models such as ours to be retrained or extended, or for independent AI models to be developed, to automatically identify early signs of bleaching. This would provide a valuable tool for timely conservation interventions and for tracking the resilience of seagrass ecosystems under climate change.

Indeed, a promising direction for future work is to extend the present framework beyond mapping the extent of *Posidonia oceanica* meadows to detect potential signals of habitat degradation. The methodology developed here provides the basis for consistently mapping seagrass distribution on an annual basis, enabling the construction of time series and the evaluation of long-term changes in extent. Such datasets are essential for assessing degradation trajectories and pinpointing areas that require closer examination. In addition, following theoretical and empirical studies that have linked spatial patterns to ecosystem health (Ruiz-Reynés et al., 2017, 2023), complementary approaches that use the spatial organization of meadows as a proxy for ecological conditions can be developed (Giménez-Romero et al., 2025a). By combining the pixel-level classification of *Posidonia oceanica* with convolutional neural networks trained for spatial pattern recognition, these approaches can help distinguish between continuous meadows and more fragmented states, such as those with striped or spotted patterns. These developments have the potential to broaden the utility of satellite-based deep learning models, providing complementary information that may be useful for monitoring seagrass conditions and supporting conservation-oriented assessments. Another possible line of work is to relate the spatial extent of *P. oceanica* meadows to temperature-based metrics (Giménez-Romero et al., 2025b). Because our model can be used to map meadows in different areas of the Mediterranean Sea, with associated prediction errors that provide constraints on the estimates, it becomes possible to compare seagrass distribution across regions and relate these patterns to thermal stress indicators. This type of analysis may help clarify the role of temperature in driving regional differences in meadow extent and contribute to a better understanding of how climate change affects the resilience of Mediterranean seagrass ecosystems.

5. Conclusion

This study represents a significant step forward in marine habitat monitoring by combining multispectral satellite imagery with deep convolutional neural networks to map *Posidonia oceanica* meadows. By leveraging an extensive and detailed georeferenced habitat dataset, we developed and benchmarked a framework that moves beyond the proof-of-concept stage and demonstrates real-world applicability. Unlike previous efforts, which were limited to single images or simplified classifiers, our approach relies on a comprehensive dataset spanning multiple regions and environmental conditions, thereby enhancing robustness and reliability. A key finding was the ability of our models to generalize across the Balearic Islands: although trained exclusively on Mallorca, they successfully predicted seagrass distribution in Ibiza, Formentera, and Menorca, where benthic habitats and optical properties differ substantially. This result highlights the transferability of the model and underscores its potential to deliver reliable estimates of habitat extent, even in areas with limited training data. Importantly, we quantified the prediction errors and demonstrated how they vary with meadow size and depth, thereby providing transparency regarding the approach's strengths and limitations.

The integration of remote sensing and deep learning has considerable implications for biodiversity monitoring and conservation. Our framework provides a scalable and cost-effective tool for generating seagrass distribution maps at operational scales and regular temporal intervals, thereby facilitating the detection of habitat degradation and assessing ecosystem resilience. By making the trained models openly available, we encourage their use and improvement by other researchers and practitioners, thereby supporting regional monitoring efforts across the Mediterranean. More broadly, this study demonstrates how AI and Earth observation can be integrated to provide actionable information for conservation, offering a pathway toward near-real-time monitoring of vulnerable ecosystems in the context of global change. Such approaches are becoming increasingly critical for timely intervention, the sustainable management of coastal habitats, and the preservation of biodiversity and ecosystem services for future generations.

CRediT authorship contribution statement

Àlex Giménez-Romero: Writing – review & editing, Writing – original draft, Visualization, Validation, Software, Methodology, Investigation, Data curation, Conceptualization. **Dhafer Ferchichi:** Writing – review & editing, Software, Methodology, Investigation, Data curation. **Pablo Moreno-Spiegelberg:** Writing – review & editing, Investigation. **Tomàs Sintes:** Writing – review & editing, Supervision, Project administration, Funding acquisition, Conceptualization. **Manuel A. Matías:** Writing – review & editing, Supervision, Project administration, Funding acquisition, Conceptualization.

Data and code availability

The final fully trained deep learning models employed to build CAMELE are available at Giménez-Romero (2024b). Because satellite imagery was obtained from Planet under the Education and Research Program, which provides limited, non-commercial access to PlanetScope and RapidEye imagery, we cannot share the raw data. However, we provide two processed images together with the ground truth data and a code example to perform predictions with the final trained models (Giménez-Romero, 2024b). A web-based application for interactively visualizing all model predictions, together with the ground truth data, is available at Giménez-Romero (2024a).

Declaration of competing interest

The authors declare that they have no known competing financial interests or personal relationships that could have appeared to influence the work reported in this paper.

Acknowledgments

This work was supported through grants TED2021-131836B-I00 (SEDIMENT) funded by Spanish Ministry of Science and Innovation MICIU/AEI/10.13039/501100011033 and by the European Union NextGenerationEU/PRTR Program; PID2021-123723OB-C22 (CYCLE) and PID2024-156062OB-I00 (CHANGE-ME) funded by MICIU/AEI/10.13039/501100011033 and by ERDF, EU; CEX2021-001164-M (María de Maeztu Program for Units of Excellence in R&D) funded by MICIU/AEI/10.13039/501100011033. We acknowledge Nuria Marbà for her valuable initial comments and suggestions. We acknowledge Marcial Bardolet and Jorge Moreno, from the Species Protection Service of the Government of the Balearic Islands, who provided the habitat data used in this study. We also acknowledge Planet Labs for access to satellite imagery data under their Education and Research Program. We express our heartfelt gratitude to José Luis Cantero Rada for being a profound source of inspiration.

Appendix A. Supplementary data

Supplementary material related to this article can be found online at https://doi.org/10.1016/j.ecolind.2025.114349.

Data availability

All data and code, except those with commercial restriction, are available in a public Zenodo repository.

References

Allen Coral Atlas, 2022. Imagery, maps and monitoring of the world's tropical coral reefs. https://zenodo.org/record/6622015.

Amani, M., Macdonald, C., Salehi, A., Mahdavi, S., Gullage, M., 2022. Marine habitat mapping using bathymetric LiDAR data: A case study from Bonne Bay, Newfoundland. Water 14 (23), http://dx.doi.org/10.3390/w14233809.

Ariasari, A., Hartono, Wicaksono, P., 2019. Random forest classification and regression for seagrass mapping using PlanetScope image in labuan bajo, east nusa tenggara. In: Setiawan, Y., Prasetyo, L.B., Pham, T.D., Kanniah, K.D., Murayama, Y., Arai, K., Perez, G.J.P. (Eds.), Sixth International Symposium on LAPAN-IPB Satellite. Vol. 11372, International Society for Optics and Photonics, p. 113721Q. http://dx.doi.org/10.1117/12.2541718.

Bakirman, T., Gumusay, M.U., 2020. Assessment of machine learning methods for seagrass classification in the mediterranean. Balt. J. Mod. Comput. 8, 315–326. http://dx.doi.org/10.22364/BJMC.2020.8.2.07.

Beck, M.W., Heck, K.L., Able, K.W., Childers, D.L., Eggleston, D.B., Gillanders, B.M., Halpern, B., Hays, C.G., Hoshino, K., Minello, T.J., Orth, R.J., Sheridan, P.F., Weinstein, M.P., 2001. The identification, conservation, and management of estuarine and marine nurseries for fish and invertebrates. Bioscience 51 (8), 633–641. http://dx.doi.org/10.1641/0006-3568(2001)051[0633:TICAMO]2.0.CO;2.

Bos, A.R., Bouma, T.J., de Kort, G.L., van Katwijk, M.M., 2007. Ecosystem engineering by annual intertidal seagrass beds: Sediment accretion and modification. Estuar. Coast. Shelf Sci. 74 (1), 344–348. http://dx.doi.org/10.1016/j.ecss.2007.04.006.

Boyle, S.A., Kennedy, C.M., Torres, J., Colman, K., Pérez-Estigarribia, P.E., de la Sancha, N.U., 2014. High-resolution satellite imagery is an important yet underutilized resource in conservation biology. PLoS One 9 (1), e86908. http://dx.doi.org/10.1371/journal.pone.0086908.

Burkholder, J.M., Tomasko, D.A., Touchette, B.W., 2007. Seagrasses and eutrophication. J. Exp. Mar. Biol. Ecol. 350 (1), 46–72. http://dx.doi.org/10.1016/j.jembe.2007.06.024, The Biology and Ecology of Seagrasses.

Chand, S., Bollard, B., 2022. Detecting the spatial variability of seagrass meadows and their consequences on associated macrofauna benthic activity using novel drone technology. Remote. Sens. 14 (1), 160. http://dx.doi.org/10.3390/rs14010160.

Chaurasia, A., Culurciello, E., 2017. LinkNet: Exploiting encoder representations for efficient semantic segmentation. In: 2017 IEEE Visual Communications and Image Processing. VCIP, IEEE, http://dx.doi.org/10.1109/vcip.2017.8305148.

Chowdhury, M., Martínez-Sansigre, A., Mole, M., Peleato, E.A., Basos, N., Blanco, J.M., Ramirez, M., Caballero, I., de la Calle, I., 2024. AI-driven remote sensing enhances Mediterranean seagrass monitoring and conservation to combat climate change and anthropogenic impacts. Sci. Rep. 14, 8360. http://dx.doi.org/10.1038/s41598-024-59091-7.

Coffer, M.M., Schaeffer, B.A., Zimmerman, R.C., Hill, V., Li, J., Islam, K.A., Whitman, P.J., 2020. Performance across WorldView-2 and RapidEye for reproducible seagrass mapping. Remote Sens. Environ. 250, 112036. http://dx.doi.org/10.1016/j.rse.2020.112036.

Dai, J., He, K., Sun, J., 2016. Instance-aware semantic segmentation via multi-task network cascades. In: Proceedings of the IEEE Conference on Computer Vision and Pattern Recognition. pp. 3150–3158. http://dx.doi.org/10.1109/CVPR.2016.343.

van de Vijsel, R.C., Hernández-García, E., Orfila, A., Gomila, D., 2023. Optimal wave reflection as a mechanism for seagrass self-organization. Sci. Rep. 13 (1), 20278. http://dx.doi.org/10.1038/s41598-023-46788-4.

Dice, L.R., 1945. Measures of the amount of ecologic association between species. Ecology 26 (3), 297–302. http://dx.doi.org/10.2307/1932409.

Doughty, C.L., Cavanaugh, K.C., Chapman, S., Fatoyinbo, L., 2024. Uncovering mangrove range limits using very high resolution satellite imagery to detect fine-scale mangrove and saltmarsh habitats in dynamic coastal ecotones. Remote. Sens. Ecol. Conserv. 10 (6), 686–701. http://dx.doi.org/10.1002/rse2.394.

Duarte, C.M., Chiscano, C.L., 1999. Seagrass biomass and production: a reassessment. Aquat. Bot. 65 (1), 159–174. http://dx.doi.org/10.1016/S0304-3770(99)00038-8.

Duarte, C.M., Losada, I.J., Hendriks, I.E., Mazarrasa, I., Marbà, N., 2013. The role of coastal plant communities for climate change mitigation and adaptation. Nat. Clim. Chang. 3 (1), 961–968. http://dx.doi.org/10.1038/nclimate1970.

Fonseca, M.S., Cahalan, J.A., 1992. A preliminary evaluation of wave attenuation by four species of seagrass. Estuar. Coast. Shelf Sci. 35 (6), 565–576. http://dx.doi.org/10.1016/S0272-7714(05)80039-3.

Fornes, A., Basterretxea, G., Orfila, A., Jordi, A., Alvarez, A., Tintore, J., 2006. Mapping *Posidonia oceanica* from IKONOS. ISPRS J. Photogramm. Remote Sens. 60 (5), 315–322. http://dx.doi.org/10.1016/j.isprsjprs.2006.04.002.

Gacia, E., Duarte, C., 2001. Sediment retention by a Mediterranean *Posidonia oceanica* meadow: The balance between deposition and resuspension. Estuar. Coast. Shelf Sci. 52 (4), 505–514. http://dx.doi.org/10.1006/ecss.2000.0753.

Gera, A., Pagès, J.F., Romero, J., Alcoverro, T., 2013. Combined effects of fragmentation and herbivory on Posidonia oceanica seagrass ecosystems. J. Ecol. 101 (4), 1053–1061. http://dx.doi.org/10.1111/1365-2745.12109.

Giménez-Romero, A., 2024a. http://camele.ifisc.uib-csic.es.

Giménez-Romero, A., 2024b. CAMELE: Consensus for automated marine ecosystem labelling and evaluation. http://dx.doi.org/10.5281/zenodo.10792281.

Giménez-Romero, À., del Campo, E., Matías, M.A., 2025a. Monitoring the resilience of seagrass meadows from satellite imagery using machine learning. Manuscript in preparation.

Giménez-Romero, À., Sintes, T., Matías, M.A., 2025b. Thermal stress drives seagrass fragmentation in the Mediterranean sea. Manuscript in preparation.

Goverment of the Balearic Islands, 2000-2019. Atlas posidonia. Cartographic data provided by Projects: LIFE NATURA 2000 (LIFE 00/NAT/E/7303), https://lifeposidonia.caib.es/user/home.htm and ATLAS POSIDONIA (ITS2017-069), https://atlasposidonia.com/en/conservation-in-the-balearic-islands/.

Granata, T.C., Serra, T., Colomer, J., Casamitjana, X., Duarte, C.M., Gacia, E., 2001. Flow and particle distributions in a nearshore seagrass meadow before and after a storm. Mar. Ecol. Prog. Ser. 218, 95–106. http://dx.doi.org/10.3354/meps218095.

Gudžius, P., Kurasova, O., Darulis, V., Filatovas, E., 2021. Deep learning-based object recognition in multispectral satellite imagery for real-time applications. Mach. Vis. Appl. 32 (4), 98. http://dx.doi.org/10.1007/s00138-021-01209-2.

Ha, N.T., Manley-Harris, M., Pham, T.D., Hawes, I., 2020. A comparative assessment of ensemble-based machine learning and maximum likelihood methods for mapping seagrass using sentinel-2 imagery in tauranga harbor, New Zealand. Remote. Sens. 12 (3), 355. http://dx.doi.org/10.3390/rs12030355.

Heck Jr, K.L., Hays, G., Orth, R.J., 2003. Critical evaluation of the nursery role hypothesis for seagrass meadows. Mar. Ecol. Prog. Ser. 253, 123–136. http://dx.doi.org/10.3354/meps253123.

van der Heide, T., van Nes, E.H., Geerling, G.W., Smolders, A.J.P., Bouma, T.J., van Katwijk, M.M., 2007. Positive feedbacks in seagrass ecosystems: Implications for success in conservation and restoration. Ecosystems 10 (8), 1311–1322. http://dx.doi.org/10.1007/s10021-007-9099-7.

Iakubovskii, P., 2019. Segmentation models. https://github.com/qubvel/segmentation_models.

Islam, K.A., Hill, V., Schaeffer, B., Zimmerman, R., Li, J., 2019. Semi-supervised adversarial domain adaptation for seagrass detection in multispectral images. In: 2019 IEEE International Conference on Data Mining. ICDM, pp. 1120–1125. http://dx.doi.org/10.1109/ICDM.2019.00134.

Jeon, E., Kim, S., Park, S., Kwak, J., Choi, I., 2021. Semantic segmentation of seagrass habitat from drone imagery based on deep learning: A comparative study. Ecol. Inform. 66, 101430. http://dx.doi.org/10.1016/j.ecoinf.2021.101430.

Jorda, G., Marbà, N., Bennett, S., Santana-Garcon, J., Agusti, S., Duarte, C.M., 2020. Ocean warming compresses the three-dimensional habitat of marine life. Nat. Ecol. Evol. 4, 109–114. http://dx.doi.org/10.1038/s41559-019-1058-0.

Kallesøe, M.F., Bambaradeniya, C.N.B., Iftikhar, U.A., Ranasinghe, T., Miththapala, S., 2008. Linking Coastal Ecosystems and Human Well-Being: Learning from Conceptual Frameworks and Empirical Results. Ecosystems and Livelihoods Group, Asia, IUCN, Colombo, https://portals.iucn.org/library/efiles/documents/2008-021.pdf.

Kellaris, A., Gil, A., Faria, J., Amaral, R., Moreu-Badia, I., Neto, A., Yesson, C., 2019. Using low-cost drones to monitor heterogeneous submerged seaweed habitats: A case study in the Azores. Aquat. Conserv.: Mar. Freshw. Ecosyst. 29, 1909–1922. http://dx.doi.org/10.1002/aqc.3189.

Kobryn, H.T., Wouters, K., Beckley, L.E., Heege, T., 2013. Ningaloo reef: Shallow marine habitats mapped using a hyperspectral sensor. PLoS ONE 8 (7), 1–22. http://dx.doi.org/10.1371/journal.pone.0070105.

Koch, E.W., Ackerman, J.D., Verduin, J., Keulen, M.v., 2006. Fluid dynamics in seagrass ecology—from molecules to ecosystems. In: Larkum, A.W.D., Orth, R.J., Duarte., C.M. (Eds.), Seagrasses: Biology, Ecology and Conservation. Springer, Dordrecht, NL, pp. 193–225. http://dx.doi.org/10.1007/978-1-4020-2983-7_8.

Le Quilleuc, A., Collin, A., Jasinski, M.F., Devillers, R., 2022. Very high-resolution satellite-derived bathymetry and habitat mapping using Pleiades-1 and ICESat-2. Remote. Sens. 14 (1), 133. http://dx.doi.org/10.3390/rs14010133.

Lin, T.-Y., Dollár, P., Girshick, R., He, K., Hariharan, B., Belongie, S., 2017. Feature pyramid networks for object detection. In: 2017 IEEE Conference on Computer Vision and Pattern Recognition. CVPR, pp. 936–944. http://dx.doi.org/10.1109/CVPR.2017.106.

Llabrés, E., Blanco-Magadán, A., Sales, M., Sintes, T., 2023. Effect of global warming on Western Mediterranean seagrasses: a preliminary agent-based modelling approach. Mar. Ecol. Prog. Ser. 710, 43–56. http://dx.doi.org/10.3354/meps14298.

Lyons, M.B., et al., 2020. Mapping the world's coral reefs using a global multiscale earth observation framework. Remote. Sens. Ecol. Conserv. 6 (4), 557–568. http://dx.doi.org/10.1002/rse2.157.

Macreadie, P., Baird, M., Trevathan-Tackett, S., Larkum, A., Ralph, P., 2014. Quantifying and modelling the carbon sequestration capacity of seagrass meadows – a critical assessment. Marine Poll. Bull. 83 (2), 430–439. http://dx.doi.org/10.1016/j.marpolbul.2013.07.038.

Madsen, J.D., Chambers, P.A., James, W.F., Koch, E.W., Westlake, D.F., 2001. The interaction between water movement, sediment dynamics and submersed macrophytes. Hydrobiologia 444, 71–84. http://dx.doi.org/10.1023/A:1017520800568.

Marbà, N., Duarte, C.M., Holmer, M., Martínez, R., Basterretxea, G., Orfila, A., Jordi, A., Tintoré, J., 2002. Effectiveness of protection of seagrass (*Posidonia oceanica*) populations in Cabrera National Park (Spain). Environ. Conserv. 29 (4), 509–518. http://dx.doi.org/10.1017/S037689290200036X.

Marcello, J., Eugenio, F., Martín, J., Marqués, F., 2018. Seabed mapping in coastal shallow waters using high resolution multispectral and hyperspectral imagery. Remote. Sens. 10, 1208. http://dx.doi.org/10.3390/rs10081208.

Martín Míguez, B., et al., 2019. The European marine observation and data network (EMODnet): Visions and roles of the gateway to marine data in europe. Front. Mar. Sci. 6 (313), 24. http://dx.doi.org/10.3389/fmars.2019.00313.

Mcleod, E., Chmura, G.L., Bouillon, S., Salm, R., Björk, M., Duarte, C.M., Lovelock, C.E., Schlesinger, W.H., Silliman, B.R., 2011. A blueprint for blue carbon: toward an improved understanding of the role of vegetated coastal habitats in sequestering CO_2. Front. Ecol. Environ. 9 (10), 552–560. http://dx.doi.org/10.1890/110004.

Mederos-Barrera, A., Marcello, J., Eugenio, F., Hernández, E., 2022. Seagrass mapping using high resolution multispectral satellite imagery: A comparison of water column correction models. Int. J. Appl. Earth Obs. Geoinf. 113, 102990. http://dx.doi.org/10.1016/j.jag.2022.102990.

Millennium Ecosystem Assessment, 2005. Ecosystems and Human Well-being: a Framework Working Group for Assessment Report of the Millennium Ecosystem Assessment. Island Press, Washington, https://www.millenniumassessment.org/documents/document.356.aspx.pdf.

Milletari, F., Navab, N., Ahmadi, S.-A., 2016. V-Net: Fully convolutional neural networks for volumetric medical image segmentation. In: 2016 Fourth International Conference on 3D Vision (3DV). pp. 565–571. http://dx.doi.org/10.1109/3DV.2016.79.

Mishra, D., Narumalani, S., Rundquist, D., Lawson, M., 2006. Benthic habitat mapping in tropical marine environments using QuickBird multispectral data. Photogramm. Eng. Remote Sens. 72, 1037–1048. http://dx.doi.org/10.14358/PERS.72.9.1037.

Montefalcone, M., Parravicini, V., Vacchi, M., Albertelli, G., Ferrari, M., Morri, C., Bianchi, C.N., 2010. Human influence on seagrass habitat fragmentation in NW Mediterranean Sea. Estuar. Coast. Shelf Sci. 86 (2), 292–298. http://dx.doi.org/10.1016/j.ecss.2009.11.018.

Mumby, P.J., Edwards, A.J., 2002. Mapping marine environments with IKONOS imagery: enhanced spatial resolution can deliver greater thematic accuracy. Remote Sens. Environ. 82 (2), 248–257. http://dx.doi.org/10.1016/S0034-4257(02)00041-X.

Planet Team, 2017. Planet Application Program Interface: In Space for Life on Earth. San Francisco, CA, https://api.planet.com.

Poursanidis, D., Topouzelis, K., Chrysoulakis, N., 2018. Mapping coastal marine habitats and delineating the deep limits of the Neptune's seagrass meadows using very high resolution earth observation data. Int. J. Remote Sens. 39, 8670–8687. http://dx.doi.org/10.1080/01431161.2018.1490974.

Poursanidis, D., Traganos, D., Reinartz, P., Chrysoulakis, N., 2019. On the use of Sentinel-2 for coastal habitat mapping and satellite-derived bathymetry estimation using downscaled coastal aerosol band. Int. J. Appl. Earth Obs. Geoinf. 80, 58–70. http://dx.doi.org/10.1016/j.jag.2019.03.012.

Rahman, M.A., Wang, Y., 2016. Optimizing intersection-over-union in deep neural networks for image segmentation. In: Bebis, G., Boyle, R., Parvin, B., Koracin, D., Porikli, F., Skaff, S., Entezari, A., Min, J., Iwai, D., Sadagic, A., Scheidegger, C., Isenberg, T. (Eds.), Advances in Visual Computing. Springer International Publishing, Cham, pp. 234–244. http://dx.doi.org/10.1007/978-3-319-50835-1_22.

Ronneberger, O., Fischer, P., Brox, T., 2015. U-Net: Convolutional networks for biomedical image segmentation. In: Navab, N., Hornegger, J., Wells, W.M., Frangi, A.F. (Eds.), Medical Image Computing and Computer-Assisted Intervention – MICCAI 2015. Springer International Publishing, Cham, pp. 234–241. http://dx.doi.org/10.48550/arXiv.1505.04597.

Ruiz-Reynés, D., Gomila, D., Sintes, T., Hernández-García, E., Marbà, N., Duarte, C.M., 2017. Fairy circle landscapes under the sea. Sci. Adv. 3 (8), e1603262. http://dx.doi.org/10.1126/sciadv.1603262.

Ruiz-Reynés, D., Mayol, E., Sintes, T., Hendriks, I.E., Hernández-García, E., Duarte, C.M., Marbà, N., Gomila, D., 2023. Self-organized sulfide-driven traveling pulses shape seagrass meadows. Proc. Natl. Acad. Sci. 120 (3), e2216024120. http://dx.doi.org/10.1073/pnas.2216024120.

Sánchez-González, J.F., Sánchez-Rojas, V., Memos, C.D., 2011. Wave attenuation due to *Posidonia oceanica* meadows. J. Hydraul. Res. 49 (4), 503–514. http://dx.doi.org/10.1080/00221686.2011.552464.

Senecal, J.J., Sheppard, J.W., Shaw, J.A., 2019. Efficient convolutional neural networks for multi-spectral image classification. In: 2019 International Joint Conference on Neural Networks. IJCNN, pp. 1–8. http://dx.doi.org/10.1109/IJCNN.2019.8851840.

Short, F.T., Wyllie-Echeverria, S., 1996. Natural and human-induced disturbance of seagrasses. Environ. Conserv. 23 (1), 17–27. http://dx.doi.org/10.1017/S0376892900038212.

Sorensen, T., 1948. A method of establishing groups of equal amplitude in plant sociology based on similarity of species content and its application to analyses of the vegetation on Danish commons. Biologiske Skr. 5, 1–34.

Stipcich, P., Arena, C., Ceccherelli, G., Donadio, R., Jimenez, C., La Manna, G., Resaikos, V., Vitale, E., Fraschetti, S., 2025a. Not only corals: seagrass bleaching in the eastern Mediterranean. Sci. Total Environ. 985, 179754. http://dx.doi.org/10.1016/j.scitotenv.2025.179754.

Stipcich, P., Arena, C., Ceccherelli, G., Donadio, R., Jimenez, C., Resaikos, V., Vitale, E., Fraschetti, S., 2025b. *Posidonia oceanica* leaf bleaching: does it affect the plant photoprotective mechanisms? Environ. Res. 284, 122233. http://dx.doi.org/10.1016/j.envres.2025.122233.

Swadling, D.S., West, G.J., Gibson, P.T., Laird, R.J., Glasby, T.M., 2023. Don't go breaking apart: Anthropogenic disturbances predict meadow fragmentation of an endangered seagrass. Aquat. Conserv.: Mar. Freshw. Ecosyst. 33 (1), 56–69. http://dx.doi.org/10.1002/aqc.3905.

Telesca, L., et al., 2015. Seagrass meadows (*Posidonia oceanica*) distribution and trajectories of change. Sci. Rep. 5 (1), 12505. http://dx.doi.org/10.1038/srep12505.

Traganos, D., Aggarwal, B., Poursanidis, D., Topouzelis, K., Chrysoulakis, N., Reinartz, P., 2018. Towards Global-Scale Seagrass Mapping and Monitoring Using Sentinel-2 on Google Earth Engine: The case study of the Aegean and Ionian seas. Remote. Sens. 10 (8), 1227. http://dx.doi.org/10.3390/rs10081227.

Traganos, D., Reinartz, P., 2018a. Machine learning-based retrieval of benthic reflectance and *Posidonia oceanica* seagrass extent using a semi-analytical inversion of Sentinel-2 satellite data. Int. J. Remote Sens. 39, 9428–9452. http://dx.doi.org/10.1080/01431161.2018.1519289.

Traganos, D., Reinartz, P., 2018b. Mapping Mediterranean seagrasses with Sentinel-2 imagery. Marine Poll. Bull. 134, 197–209. http://dx.doi.org/10.1016/j.marpolbul.2017.06.075.

2012. United Nations Conference on Sustainable Development, Rio+20. URL https://sustainabledevelopment.un.org/rio20. (visited on 12/12/2024).

del Valle Villalonga, L., Pons, G.X., Bardolet, M., 2023. *Posidonia oceanica* cartography and evolution of the Balearic sea (Western Mediterranean). Remote. Sens. 15 (24), 5748. http://dx.doi.org/10.3390/rs15245748.

Waltham, N.J., et al., 2022. UN decade on ecosystem restoration 2021–2030—What chance for success in restoring co astal ecosystems? Front. Mar. Sci. 7, 71. http://dx.doi.org/10.3389/fmars.2020.00071.

Waycott, M., et al., 2009. Accelerating loss of seagrasses across the globe threatens coastal ecosystems. Proc. Natl. Acad. Sci. U.S.A. 106 (30), 12377–12381. http://dx.doi.org/10.1073/pnas.0905620106.

Wicaksono, P., Aryaguna, P.A., Lazuardi, W., 2019. Benthic habitat mapping model and cross validation using machine-learning classification algorithms. Remote. Sens. 11 (11), 1279. http://dx.doi.org/10.3390/rs11111279.

Wilson, K.L., Wong, M.C., Devred, E., 2022. Comparing Sentinel-2 and WorldView-3 imagery for coastal bottom habitat mapping in Atlantic Canada. Remote. Sens. 14 (5), http://dx.doi.org/10.3390/rs14051254.

Yang, C., Yang, D., Cao, W., Zhao, J., Wang, G., Sun, Z., Xu, Z., Ravi Kumar, M., 2010. Analysis of seagrass reflectivity by using a water column correction algorithm. Int. J. Remote Sens. 31 (17–18), 4595–4608. http://dx.doi.org/10.1080/01431161.2010.485138.

Zeiler, M.D., Fergus, R., 2014. Visualizing and understanding convolutional networks. In: Fleet, D., Pajdla, T., Schiele, B., Tuytelaars, T. (Eds.), Computer Vision – ECCV 2014. Springer International Publishing, Cham, pp. 818–833. http://dx.doi.org/10.1007/978-3-319-10590-1_53.

Zhang, C., Selch, D., Xie, Z., Roberts, C., Cooper, H., Chen, G., 2013. Object-based benthic habitat mapping in the Florida keys from hyperspectral imagery. Estuar. Coast. Shelf Sci. 134, 88–97. http://dx.doi.org/10.1016/j.ecss.2013.09.018.

Zhang, Y., Yu, X., Chen, Z., Wang, Q., Zuo, J., Yu, S., Guo, R., 2023. A review of seagrass bed pollution. Water 15 (21), http://dx.doi.org/10.3390/w15213754.

Zhao, H., Shi, J., Qi, X., Wang, X., Jia, J., 2017. Pyramid scene parsing network. In: 2017 IEEE Conference on Computer Vision and Pattern Recognition. CVPR, pp. 6230–6239. http://dx.doi.org/10.1109/CVPR.2017.660.

Zoffoli, M.L., Frouin, R., Kampel, M., 2014. Water column correction for coral reef studies by remote sensing. Sensors 14 (9), 16881–16931. http://dx.doi.org/10.3390/s140916881.